**Supporting Information**

# Photochemical Aging of Beijing Urban $PM_{2.5}$: HONO Production

Fengxia Bao [a,b], Meng Li [a,b] , Yue Zhang [a,b], Chuncheng Chen [a,b,*], Jincai Zhao [a,b]

[a] *Key Laboratory of Photochemistry, CAS Research/Education Center for Excellence in Molecular Sciences, Institute of Chemistry, Chinese Academy of Sciences, Beijing, 100190, P. R. China*

[b] University of Chinese Academy of Sciences, Beijing, 100049, P. R. China

Corresponding Authors:

Prof. Chuncheng Chen Email: ccchen@iccas.ac.cn

# Table of Contents

**Figure S9.**The measured $NO_3^-$ concentrations of A. freshly collected; B. photochemical aged (10 h irradiation); C photochemical aged (10 h irradiation and another 10 h irradiation with HCl flow) $PM_{2.5}$ sample (NOV28).

**Figure S10.** HONO and $NO_2$ production from the Beijing urban $PM_{2.5}$ (NOV28) with HCl flux without light irradiation.

**Figure S11.** Cumulative (a) HONO production and (b) $NO_2$ production from the Beijing urban $PM_{2.5}$ (JUL05) as a function of the irradiation time (t) at different RH values.

**Figure S12.** Cumulative HONO production from the Beijing urban $PM_{2.5}$ (NOV16) as a function of (a) light intensity and (b) light wavelength; all experiments were conducted at RH = 60%, temperature = 25 $^oC$.

# Supplementary Methods

**Sampling and filter treatment.** The ambient fine particulate matter ($PM_{2.5}$) (aerodynamic particle size < 2.5 μm) was collected on quartz microfiber filters (Whatman, 203 mm × 254 mm) by a 600/AFPM1001K High Volume Sampler (AMS) operated at a flow rate of 0.8 ~ 1.0 $m^3$/min for 24 h. The air volume through each filter ranged from 578 to 1239 $m^3$. Samples were collected on the roof of the ten-storey building of the Institute of Chemistry, Chinese Academy of Sciences (ICCAS, 116°19'21.58''E, 39°59'22.68''N) that is located in Haidian District of Beijing, a typical heavily polluted urban area. During collection, an additional filter was placed behind the sampling filter as the exposure blank control to avoid sampling artifact signal. The samples were collected in various seasons from Apr 2016 to Dec 2016. Before sampling, the blank filters were stored in 30% RH and 25 °C. After sampling the filters were stabilized in the same RH and temperature to be weighed, after which the filters were stored at - 20 °C in the freezer. Fractions with given surface area from one randomized-chosen filters were used to perform the photochemical experiments or other analysis.

**Photoreaction system.** The gas supply system was composed of two inlet Teflon tubes. The first line supplied a mixture of ultra-high-purity nitrogen and ultra-high-purity oxygen; the second line supplied humid ultra-high-purity nitrogen through water bubbler. The ratio of total nitrogen to oxygen was 26:7. Relative humidity was monitored with an in-line RH sensor (Vaisala, HMT130). Mass flow

controllers (Beijing Sevenstar electronics Co., Ltd.) were used to adjust the gas flow. The mixed gas flow was then through a custom-made photochemical flow reactor. During the photoreaction process, a fraction of $PM_{2.5}$ sample collected on a quartz filter was exposed to simulated solar irradiation of a Xenon lamp (300W) and the water circulating bath (Beijing YKKY Technology Co., Ltd) was employed constantly ($5^oC \sim 60^oC$). Light intensity was calibrated by a CEL-NP2000 lightmeter (CEAULIGHT). Before and after the light-exposure experiment, baselines of both HONO and $NO_2$ were established. With the resident time ~ 6 s of the carrier gas in the reactor, the photolysis loss of HONO and $NO_2$ during irradiation was negligible. A control experiment was conducted by illuminating the empty flow reactor to correct for HONO and $NO_2$ generation caused by photolysis of $HNO_3$ deposited on the flow reactor wall surface.

***On-line*** **gas measurement.** Gases products HONO and $NO_x$ released during the experiment were flushed out of the reactor by the carrier gas and were detected by a MODEL T200 $NO_x$ analyzer (Teledyne API). In this analyzer, the reaction of NO with $O_3$ produces a characteristic luminescence with intensity proportional to the NO concentration, which is the basis of NO detection. A molybdenum catalyst was used to convert HONO and $NO_2$ to NO, which is used for the detection of HONO and $NO_2$. The concentration of HONO and $NO_2$ was detected by a widely-used method [1, 2]. In this method, a quartz tube (10 cm length and 0.6 cm inner diameter) filled with 1.0 g of crystalline $Na_2CO_3$ (Beijing Chemical Works, 99.8%) was used as a denuder between the exit of the flow tube reactor and the $NO_x$ analyzer. The $NO_2$ was quantified by passing the effluent flow through this carbonate denuder which traps HONO. The HONO concentration was then indirectly verified as the difference in the signal without and with the carbonate denuder. For each experiment, a new denuder was used to prevent saturation effects. The $NO_2$ interference trapped by the denuder has been corrected. Before detection of gas products, a NaCl (Beijing Chemical Works, 99.5%) denuder was used to trap $HNO_3$ which was a potential interference[3]. To eliminate the influence of the unknown dark reactions and processes, dark control experiments were also conducted. The control signals were subtracted from the sample exposure signals when calculating the production rates of HONO and $NO_2$.

**Actinometry calibration.** To adjust the $J$ value to ambient sunlight condition (solar elevation angle $\theta = 0^{o}$), the radiant output of the solar simulator was quantified by a previously developed nitrate actinometer[4] where benzoic acid (BA) serves as an ·OH scavenger for the nitrate photolysis product ·OH forming salicylic acid (SA). Sodium nitrate (≥99%) was purchased from Acros and Sodium benzoate (99%), salicylic acid (≥99%) were purchased from Alfa Aesar. The produced SA in the actinometer was quantified by a fluorescence spectrometer (Hitachi F-7000) at an excitation wavelength of 305 nm and an emission wavelength of 410 nm. The rate of SA formation is found from the plot of SA concentration as a function of time as shown in **Figure S2**. The aqueous nitrate photolysis rate in the actinometer solution exposed to the experimental light source ($J_{exp}$), was calculated by:

$$J_{\mathrm{exp}} = \frac{[\mathrm{SA}]}{[\mathrm{Nitrate}] \times \mathrm{Yield(SA)} \times \mathrm{t}}$$

where [SA], in units of M, is the measured concentration of SA in the actinometer after irradiation time(t); [Nitrate] is the concentration of nitrate added in the actinometer; Yield(SA) is the yield of SA from the reaction of ·OH radical and benzoate. To be noted, since the photolysis of homogenous nitrate and the $HNO_3$ adsorbed in $PM_{2.5}$ should have different wavelength dependences, the use of nitrate actinometry to determine the light intensity may have some uncertainty. However, by using $J_{exp}$ as a standard, the photolysis rate constants of HONO and $NO_2$ can be facilely normalized to the light intensity condition at tropical noontime and can be conveniently compared with other studies[5, 6, 7, 8].

**$HNO_3$ loading on different supports.** $HNO_3$ was introduced into the system by flowing the ultrahigh purity (UHP) nitrogen over the 16 M $HNO_3$ solution kept in a reservoir that was maintained at a constant temperature (25 $^{o}$C). The concentration of $HNO_3$ vapor was determined by IC measurement of $NO_3^-$ ions produced from dissolution of $HNO_3$ in $Na_2CO_3$ solution. The flow of UHP $N_2$ was 500 ml·min$^{-1}$ in the chamber and led to the constant $HNO_3$ vapor flow concentration between 0.11 ug/ml to 0.15 ug/ml through the sample chamber. To minimize $NO_2$ impurity in $HNO_3$, we purged $NO_2$ by bubbling the liquid $HNO_3$ for about 60 min with a steady flow of nitrogen. Before each experiment, the system was passivated with $HNO_3$ for 30 min to obtain a stable $HNO_3$ vapor concentration. The gaseous $HNO_3$ source was connected to the reactor with the supports for overnight (10 h) to make sure that the

adsorption was saturated before each photolysis experiment. The supports including $PM_{2.5}$ sample (JUL07), $Al_2O_3$ (Alfa, γ-phase 99.9%, ~40 μm), $TiO_2$ (Acros, ≥98%, ~ 4 μm), blank quartz filter and pyrex glass were tested, respectively. $PM_{2.5}$ sample, the blank quartz filter or the pyrex glass were directly placed on the bottom of the reactor, and for $Al_2O_3$ or $TiO_2$, 400 mg of this powder sample was uniformly spread on the bottom. The amount of $HNO_3$ adsorbed on the supports was quantified by washing the supports with deionized water after the irradiation, followed by detecting nitrate in the washing solution.

**The calibration of HONO measurement**. The HONO production was calibrated by IC measurement of $NO_2^-$ ions produced from dissolution of HONO. We conducted several HONO production experiments on our $PM_{2.5}$ samples with different RH values (0 ~ 60%). The gas product was simultaneously measured by $NO_x$ analyzer and IC (by the dissolution of HONO into water). The HONO concentrations in both analyses were conducted by the subtractive method of measured concentration with or without $Na_2CO_3$ denuder. The calibration results see **Figure S3**, which suggested that the measured HONO production by the $NO_x$ analyzer was nearly identical with the IC measured value. Besides, the HONO production measured by the $NO_x$ analyzer was also calibrated by a long-path absorption photometer (LOPAP) HONO analyzer. The mechanism of the LOPAP analyzer was based on the long path-length absorbance spectroscopy[9, 10, 11].

# Supplementary Tables

**Table S1.** Overview of HONO measurements in Beijing and other cities.

| Location | Date | HONO(ppb) | Unknown sources (ppbV/hr) | Ref. |
|---|---|---|---|---|
| Paris/France | Jul 2009 | 0.10–0.21 | | 12 |
| | Jan - Feb 2010 | 0.40–0.5 | | |
| Pabstthum/Germany | July - Aug 1998 | 0.20 | | 13 |
| Rome/Italy | May - June 2001 | 0.58 | | 14 |
| EI Arenosillo/Spain | Nov - Dec 2008 | 0.08 | | 15 |
| Houston/America | Sep 2006 | 0.30 | | 16 |
| Barrow/Alaska | Mar - Apr 2009 | 0.03 | | 17 |
| Ontario/Canada | Jun - Jul 2007 | 0.06 (Day)<br>0.10 (Night) | | 18 |
| Tokyo/Japan | Jan - Feb 2004 | 0.43 | | 19 |
| Seoul/Korea | May - July 2005 | 0.36 | | 20 |

| | | | | |
|---|---|---|---|---|
| Shanghai/China | Aug 2010 - Jun 2012 | 0.92 | | [21] |
| Back Garden/China | Jun 2006 | 0.24 (Day)<br>0.95 (Night) | | [22] |
| Hong Kong/China | Aug 2011- May 2012 | 0.35-0.93 | | [23] |
| Beijing/China | Feb 2014 - Mar 2014 | 0.49-3.24 (Haze)<br>0.28-1.52 (Clean) | 1.85<br>1.26 | [24] |
| Beijing/China | Sep 2015 - Jul 2016 | 1.44 | 1.30-3.82 | [25] |
| Beijing/China | Aug 2007 | 1.45 | | [26] |
| Beijing/China | Jan - Feb 2007 | 1.04 | | [26] |
| Beijing/China | 18 - 31 Aug 2006 | 0.3-0.5 (Day)<br>0.8-3.7 (Night) | 1.0 | [27] |
| Beijing/China | Apr - Dec 2016 | | 0.12-4.57 | This work |

**Table S2.** *J* values for nitrate decay on different surfaces.

| Surface | $J_{HNO3→HONO}$($10^{-6}$ $s^{-1}$) | $J_{HNO3→NO2}$($10^{-6}s^{-1}$) | Yield ratio HONO/$NO_2$ |
|---|---|---|---|
| **$PM_{2.5}$( JUL07)** [a] | 1.77 | 0.23 | 7.70 |
| **$HNO_3$ deposited $Al_2O_3$** | 0.64 | 3.64 | 0.18 |
| **$HNO_3$ deposited $TiO_2$** | 0.65 | 3.63 | 0.18 |
| **$HNO_3$ deposited filter** | ND [b] | ND [b] | - |
| **$HNO_3$ deposited glass** | ND [b] | ND [b] | - |

[a] With pre-adsorbed $HNO_3$, $D_{NO3^-}$ is much higher. Therefore, the *J* value of Jul07 here is lower than that of the original $PM_{2.5}$ samples, as suggested in **Figure 1b.** [b] ND = Not detectable (The lower detection limit of T200 Teledyne NOx analyzer is 0.4 ppb.)

**Table S3.** Components（mass percent concentration）of different $PM_{2.5}$ samples [a]

| Item | Component | SEP05 （%） | JUL06 （%） | SEP06 （%） | DEC12 （%） | OCT13 （%） | JUL07 （%） |
|---|---|---|---|---|---|---|---|
| 1 | Element Carbon | 5.00 | 32.86 | 40.00 | 48.00 | 51.35 | 48.50 |
| 2 | Organic Carbon | 10.00 | 55.71 | 20.00 | 32.00 | 33.78 | 48.50 |
| 3[a] | $Cl^-$ | 0.82 | 0.02 | 0.29 | 0.17 | 0.15 | 0.03 |
| 4 | $NO_3^-$ | 1.06 | 0.30 | 1.03 | 0.83 | 4.31 | 0.89 |
| 5 | $SO_4^{2-}$ | 4.33 | 0.91 | 3.02 | 0.65 | 1.45 | 1.79 |

| | | | | | | | |
|---|---|---|---|---|---|---|---|
| 6 | $PO_4^{3-}$ | 2.64 | 0.08 | 0.94 | 0.23 | 0.07 | - |
| 7[b] | Al | 3.89 | 0.11 | 2.39 | 0.31 | 0.37 | 0.01 |
| 8 | Ti | 0.52 | 0.02 | 0.28 | 0.03 | 0.04 | - |
| 9 | Cr | 2.16 | 0.02 | 0.35 | 0.04 | 0.05 | 0.01 |
| 10 | Mn | 0.40 | 0.03 | 0.19 | 0.05 | 0.05 | 0.01 |
| 11 | Sn | - | 0.01 | - | - | 0.01 | - |
| 12 | Ni | - | - | 0.09 | 0 .01 | 0.00 | - |
| 13 | Cu | - | 0.02 | 0.11 | 0.02 | 0.02 | - |
| 14 | Zn | 0.39 | 0.07 | 0.52 | 0.09 | 0.11 | - |
| 15 | Ba | 0.18 | 0.01 | 0.08 | 0.02 | 0.02 | - |
| 16 | Pb | 0.27 | 0.04 | 0.31 | 0.07 | 0.07 | 0.01 |
| 17 | Ca | 2.82 | 0.09 | 5.67 | 1.61 | 1.05 | 0.03 |
| 18 | Na | 22.26 | 0.02 | 15.42 | 3.82 | 2.07 | 0.01 |
| 19 | K | 0.76 | 0.23 | 2.80 | 0.56 | 0.49 | - |
| 20 | Fe | 26.91 | 4.71 | 7.87 | 5.58 | 1.83 | 0.02 |
| 21 | Mg | 2.02 | 0.02 | 1.70 | 0.40 | 0.31 | 0.01 |
| 22 | others | 13.53 | 4.74 | -3.05 | 5.53 | 2.39 | 0.18 |

[a] Components of $PM_{2.5}$ samples: inorganic ions were measured by an ICS-900 ion chromatograph (DIONEX); metallic elements were measured by a 7700 ICP-MS (Agilent)；elemental carbon and organic carbon were measured by a Pyris-1 Thermogravimetric Analyzer (PerkinElmer) and a Nicolet iS5 ATR-IR (Thermo).

# Supplementary Figures

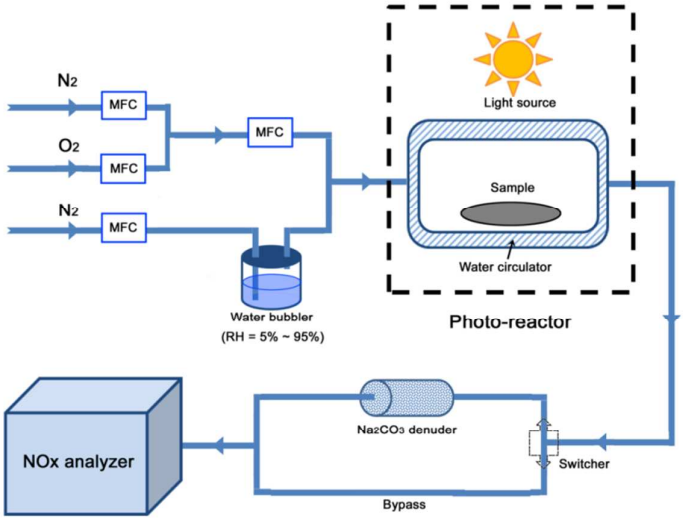


**Figure S1.** A schematic diagram of photochemical experimental setup to study the photochemical aging of urban $PM_{2.5}$.

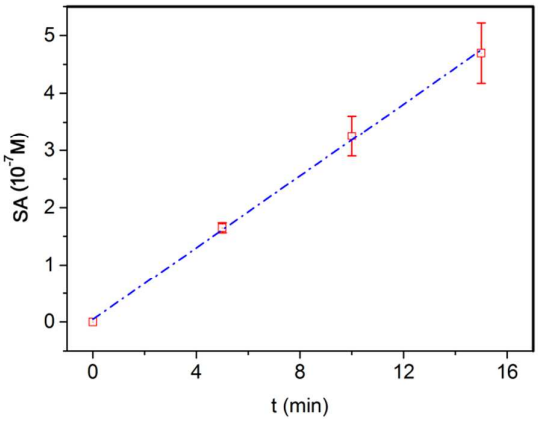


**Figure S2.** Growth of SA due to aqueous nitrate photolysis: Plot of the SA concentration as a function of reaction time (t) upon illumination of the nitrate actinometer.

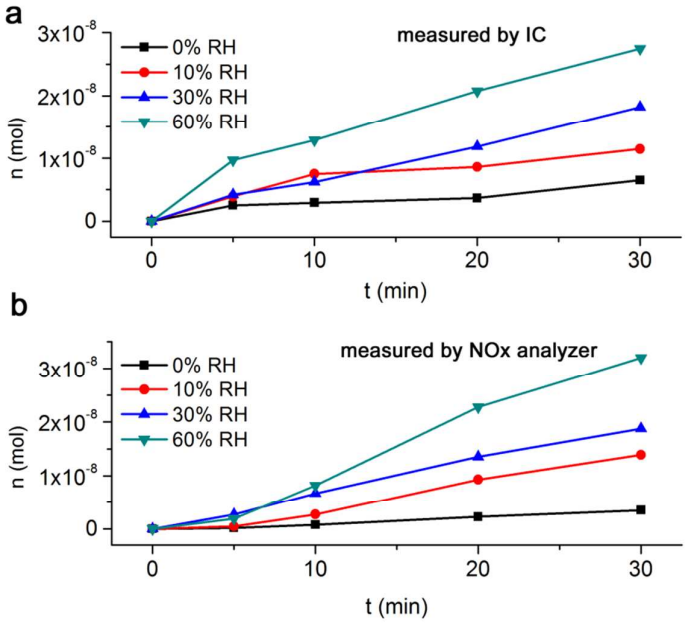

**Figure S3.** The calibration of $NO_x$ analyzer measured HONO concentration by the IC measurement of the $NO_2^-$ ions. Several HONO production experiments on the $PM_{2.5}$ sample (JUL06) with different RH values (0 ~ 60%) were conducted for 30 min. Result showed that the measured HONO production by the $NO_x$ analyzer was nearly identical with the IC measured value.

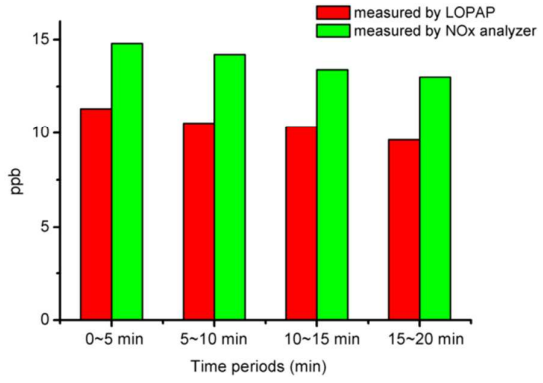


**Figure S4.** The calibration of the $NO_x$ analyzer measured HONO concentration by the LOPAP HONO analyzer. The HONO production experiments on the $PM_{2.5}$ sample (JUL06) under irradiation for different time periods were measured by both LOPAP and $NO_x$ analyzer. Result showed that the discrepancy between HONO production values measured by different methods was within 3 ppb range. The Teledyne $NO_x$ analyzer detects indirectly the HONO by using a carbonate denuder to adsorb HONO. The carbonate denuder may adsorb a small quantity of other nitrogen species (such as $N_2O_5$) which can also cause interferences when using molybdenum converters in $NO_x$

analyzer[28]. Therefore, HONO measured by $NO_x$ analyzer may be slightly higher than that by LOPAP.

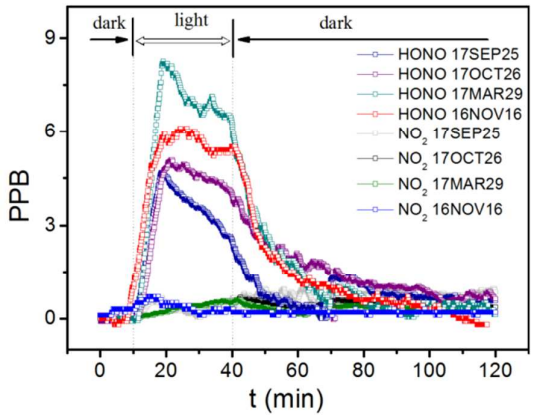


**Figure S5.** The HONO and $NO_2$ production from $PM_{2.5}$ samples during the irradiation. Samples includes 17SEP25, 17OCT26, 17MAR29 (collected in 2017) and 16NOV16(collected in 2016).

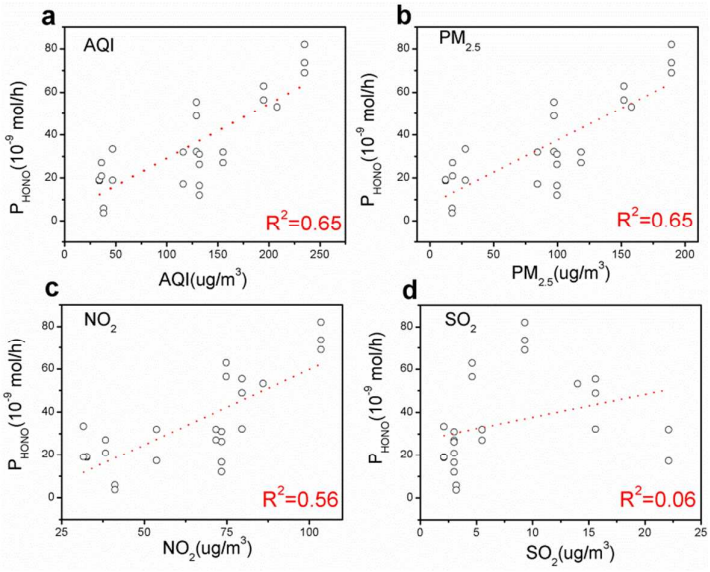


207

208 **Figure S6.** The production rates of HONO ($P_{HONO}$) as a function of **a**. AQI (Air
209 Quality index, μg/$m^3$) **b.** $PM_{2.5}$ concentration (μg/$m^3$) **c.** $NO_2$ concentration (μg/$m^3$)
210 **d.** $SO_2$ concentration (μg/$m^3$) of the day when the $PM_{2.5}$ was sampled. The
211 parameters for the weather conditions were obtained from China real-time air quality
212 monitoring and assessment platform (https://www.aqistudy.cn/historydata/).

213

214

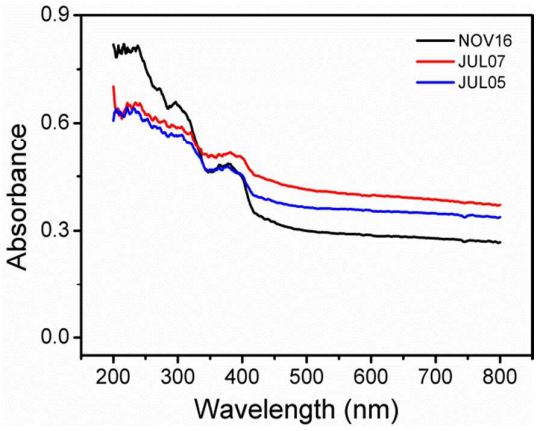


215

216 **Figure S7.** UV-Vis absorbance of $PM_{2.5}$ samples (black, Sample NOV16; red,

Sample JUL07; blue, Sample JUL05) as the function of wavelength 200 nm to 800 nm.

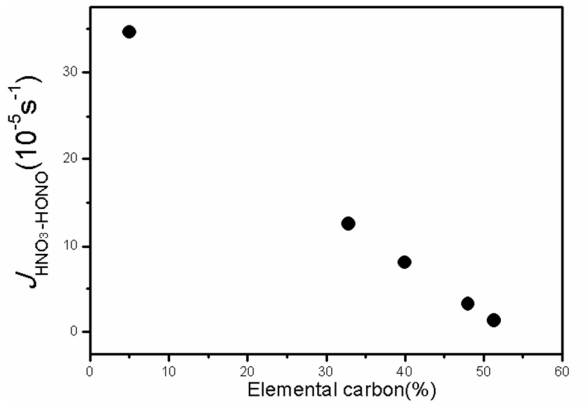


**Figure S8.** The photolysis rate constants $J_{HNO3 \rightarrow HONO}$ as a function of elemental carbon (mass percent concentration, %) of different $PM_{2.5}$ samples (RH = 60%, temperature = 25 °C).

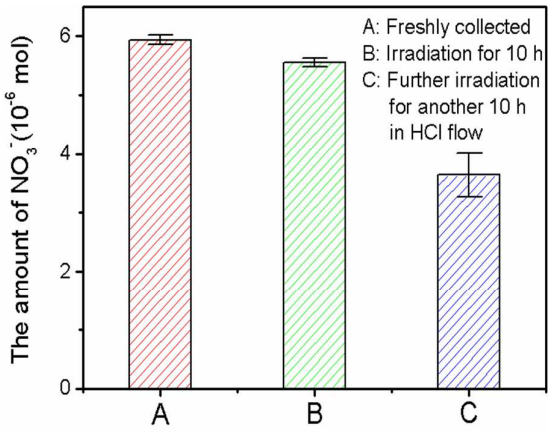

**Figure S9.** The measured $NO_3^-$ concentrations of A: freshly collected; B: photochemical aged (10 h irradiation); C: photochemical aged (further irradiation with another 10 h in HCl flow) $PM_{2.5}$ sample (NOV28). The amount of $NO_3^-$ decreased from $5.55 \times 10^{-6}$ mol to $3.64 \times 10^{-6}$ mol after irradiation of 10 h in HCl flux, which means that much more $NO_3^-$ (34%) is lost than that in the first irradiation of 10 h without HCl (5%). Besides the photoreaction, the direct evaporation of the $HNO_3$ from the $PM_{2.5}$ during the purging of HCl may also be responsible for the large loss of $NO_3^-/HNO_3$, since the nitrate ions were detected in the outlet of HCl flux.

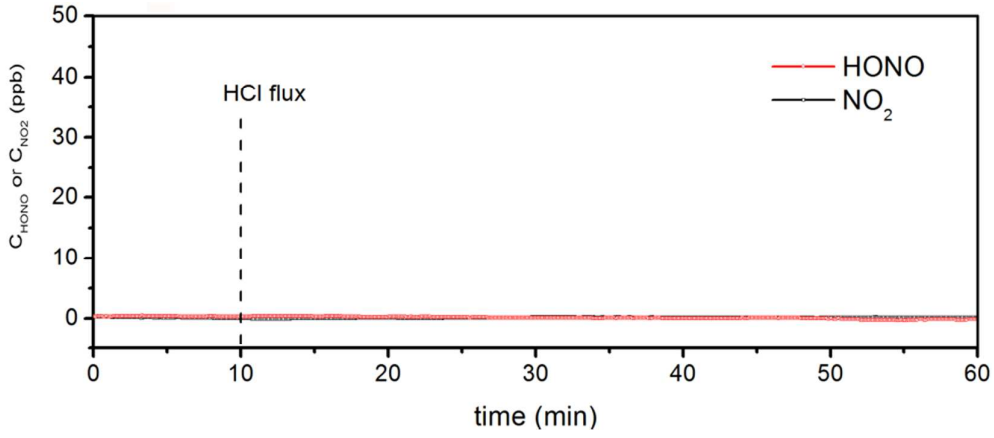


**Figure S10.** HONO and $NO_2$ production from the Beijing urban $PM_{2.5}$ (NOV28) with HCl flux without light irradiation.

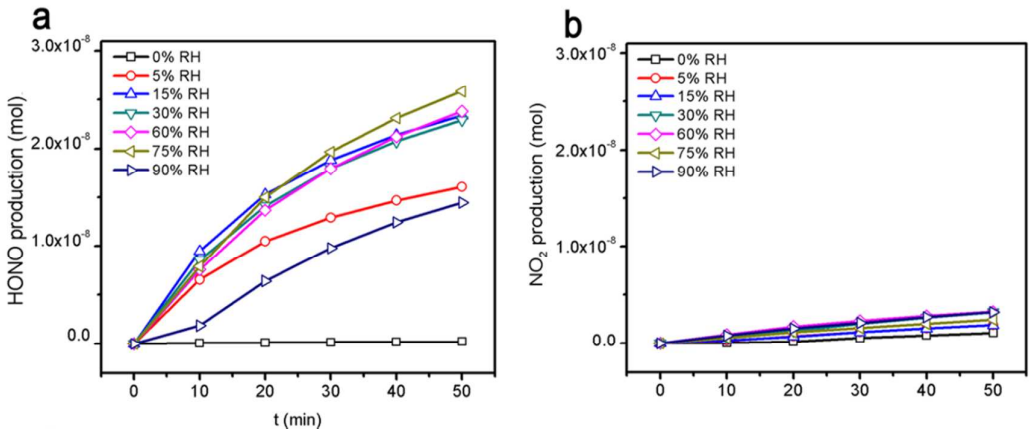


**Figure S11.** Cumulative (a) HONO production and (b) $NO_2$ production from the Beijing urban $PM_{2.5}$ (JUL05) as a function of the irradiation time (t) at different RH values.

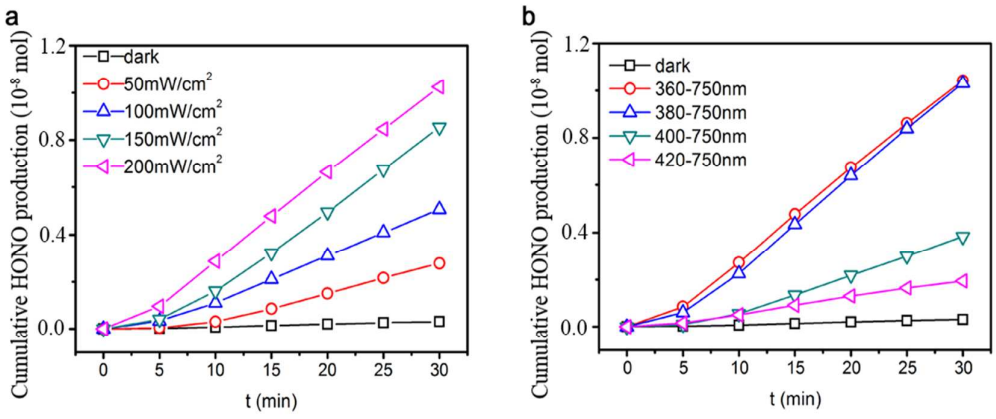


**Figure S12.** Cumulative HONO production from the Beijing urban $PM_{2.5}$ (NOV16) as a function of irradiation time at different (a) light intensity and (b) light wavelength; all experiments were conducted at RH = 60%, temperature = 25 $^{o}$C.

## References.


1. Monge, M. E.; D'Anna, B.; Mazri, L.; Giroir-Fendler, A.; Ammann, M.; Donaldson, D. J.; George, C., Light changes the atmospheric reactivity of soot. *Proc. Nat. Ac. Sci. U.S.A* **2010,** *107*, 6605-6609.

2. Han, C.; Yang, W.; Wu, Q.; Yang, H.; Xue, X., Heterogeneous Photochemical Conversion of NO2 to HONO on the Humic Acid Surface under Simulated Sunlight. *Environ. Sci. Technol.* **2016,** *50*, 5017-5023.

3. Vlasenko, A.; Huthwelker, T.; GãGgeler, H. W.; Ammann, M., Kinetics of the heterogeneous reaction of nitric acid with mineral dust particles: an aerosol flowtube study. *Phys. Chem. Chem. Phys.* **2009,** *11*, 7921-30.

4. Jankowski, J. J.; Kieber, D. J.; Mopper, K.; Neale, P. J., Development and Intercalibration of Ultraviolet Solar Actinometers. *J. Photochem. Photobiol.* **2000,** *71*, 431.

5. Baergen, A. M.; Donaldson, D. J., Photochemical renoxification of nitric acid on real urban grime. *Environ. Sci. Technol.* **2013,** *47*, 815-820.

6. Ye, C.; Gao, H.; Zhang, N.; Zhou, X., Photolysis of Nitric Acid and Nitrate on Natural and Artificial Surfaces. *Environ. Sci. Technol.* **2016,** *50*, 3530-3536.

7. Ye, C.; Zhang, N.; Gao, H.; Zhou, X., Photolysis of particulate nitrate as a source of HONO and $NO_x$. *Environ. Sci. Technol.* **2017,** *51,* 6849-6856.

8. Ye, C.; Zhou, X.; Pu, D.; Stutz, J.; Festa, J.; Spolaor, M.; Tsai, C.; Cantrell, C.; Mauldin, R. L., III; Campos, T.; Weinheimer, A.; Hornbrook, R. S.; Apel, E. C.; Guenther, A.; Kaser, L.; Yuan, B.; Karl, T.; Haggerty, J.; Hall, S.; Ullmann, K.; Smith, J. N.; Ortega, J.; Knote, C., Rapid cycling of reactive nitrogen in the marine boundary layer. *Nature* **2016,** *532*, 489-91.

9. Kleffmann, J.; Heland, J.; Kurtenbach, R.; Lörzer, J. C.; Wiesen, P., A new instrument (LOPAP) for the detection of nitrous acid (HONO). *Environ. Sci. Pollut. R.* **2002,** *9*, 48-54.

10. Huang, G.; Zhou, X.; Deng, G., Measurements of atmospheric nitrous acid and nitric acid. *Atmos. Environ.* **2002,** *36*, 2225-2235.

11. Heland, J.; Kleefmann, J.; Kurtenbach, R.; Wiesen, P., A new instrument to measure gaseous nitrous acid (HONO) in the atmosphere. *Environ. Sci. Technol.* **2001,** *35*, 3207.

12. Michoud, V.; Colomb, A.; Borbon, A.; Miet, K.; Beekmann, M.; Camredon, M.; Aumont, B.; Perrier, S.; Zapf, P.; Siour, G., Study of the unknown HONO daytime source at a European suburban site during the MEGAPOLI summer and winter field campaigns. *Atmos. Chem. Phys.* **2014,** *14*, 2805-2822.

13. licke, B.; Geyer, A.; Hofzumahaus, A.; Holland, F.; Konrad, S.; Pätz, H. W.; Schäfer, J.; Stutz, J.; Volz-Thomas, A.; Platt, U., OH formation by HONO photolysis during the BERLIOZ experiment. *J. Geophys. Res.* **2003,** *108*, PHO-1-PHO 3-17.

14. ker, K.; Febo, A.; Trick, S.; Perrino, C.; Bruno, P.; Wiesen, P.; Möller, D.; Wieprecht, W.; Auel, R.; Giusto, M., Nitrous acid in the urban area of Rome. *Atmos. Environ.* **2006,** *40*, 3123-3133.

15. Rgel, M. S.; Regelin, E.; Bozem, H.; Diesch, J. M.; Drewnick, F.; Fischer, H.; Harder, H.; Held, A.; Hosaynalibeygi, Z.; Martinez, M., Quantification of the unknown HONO daytime source and its relation to $NO_2$. *Atmos. Chem. Phys.* **2011,** *11*, 10433-10447.

16. Wong, K. W.; Oh, H. J.; Lefer, B. L.; Rappenglück, B.; Stutz, J., Vertical profiles of nitrous acid in the nocturnal urban atmosphere of Houston, TX. *Atmos. Chem. Phys. Discuss.* **2010,** *10*, 3595-3609.

17. Villena, G.; Wiesen, P.; Cantrell, C. A.; Flocke, F.; Fried, A.; Hall, S. R.; Hornbrook, R. S.;

299 Knapp, D.; Kosciuch, E.; Iii, R. L. M., Nitrous acid (HONO) during polar spring in Barrow, Alaska:
300 A net source of OH radicals? *J. Geophys. Res. Atmos.* **2011,** *116*, 191-200.
301 18. Wentzell, J. J. B.; Schiller, C. L.; Harris, G. W., Measurements of HONO during BAQS-Met.
302 *Atmos. Chem. Phys. Discuss.* **2010,** *10*, 12285-12293.
303 19. Kanaya, Y.; Cao, R.; Akimoto, H.; Fukuda, M.; Komazaki, Y.; Yokouchi, Y.; Koike, M.;
304 Tanimoto, H.; Takegawa, N.; Kondo, Y., Urban photochemistry in central Tokyo: 1. Observed and
305 modeled OH and HO2 radical concentrations during the winter and summer of 2004. *J. Geophys. Res.*
306 **2007,** *112*, D21312.
307 20. Song, C. H.; Mi, E. P.; Lee, E.; Lee, J. H.; Bo, K. L.; Dong, S. L.; Kim, J.; Han, J. S.; Moon, K. J.;
308 Kondo, Y., Possible particulate nitrite formation and its atmospheric implications inferred from the
309 observations in Seoul, Korea. *Atmos. Environ.* **2009,** *43*, 2168-2173.
310 21. Wang, S.; Zhou, R.; Zhao, H.; Wang, Z.; Chen, L.; Zhou, B., Long-term observation of
311 atmospheric nitrous acid (HONO) and its implication to local NO 2 levels in Shanghai, China. *Atmos.*
312 *Environ.* **2013,** *77*, 718-724.
313 22. Li, X.; Brauers, T.; Seler, R. H.; Bohn, B.; Fuchs, H.; Hofzumahaus, A.; Holland, F.; Lou, S.; Lu,
314 K. D.; Rohrer, F., Exploring the atmospheric chemistry of nitrous acid (HONO) at a rural site in
315 Southern China. *Atmos. Chem. Phys. Discuss.* **2011,** *11*, 27591-27635.
316 23. Xu, Z.; Wang, T.; Wu, J.; Xue, L.; Chan, J.; Zha, Q.; Zhou, S.; Louie, P. K. K.; Luk, C. W. Y.,
317 Nitrous acid (HONO) in a polluted subtropical atmosphere: Seasonal variability, direct vehicle
318 emissions and heterogeneous production at ground surface. *Atmos. Environ.* **2015,** *106*, 100-109.
319 24. Hou, S.; Tong, S.; Ge, M.; An, J., Comparison of atmospheric nitrous acid during severe haze and
320 clean periods in Beijing, China. *Atmos. Environ.* **2016,** *124*, 199-206.

321 25. Wang, J.; Zhang, X.; Guo, J.; Wang, Z.; Zhang, M., Observation of nitrous acid (HONO) in
322 Beijing, China: Seasonal variation, nocturnal formation and daytime budget. *Sci. Total Environ.* **2017,**
323 *s 587–588*, 350-359.
324 26. Spataro, F.; Ianniello, A.; Esposito, G.; Allegrini, I.; Zhu, T.; Hu, M., Occurrence of atmospheric
325 nitrous acid in the urban area of Beijing (China). *Sci. Total Environ.* **2013,** *447*, 210-224.
326 27. Qiang, Y.; Hang, S. U.; Xin, L. I.; Cheng, Y. F.; Keding, L. U.; Peng, C.; Jianwei, G. U.; Song,
327 G.; Min, H. U.; Zeng, L. M., Daytime HONO formation in the suburban area of the megacity Beijing,
328 China. *Sci. China. Chem.* **2014,** *57*, 1032-1042.
329 28. Wei, C.; Zeng, L.; Yusheng, W. U., An comparative analysis of the accuracy of atmospheric $NO_x$
330 measurements. *Acta Scien. Circum.* **2013,** *33*, 346-355.
331
332
333
334